



Journal of Smart Algorithms and Applications JSAA

ISSN: 3070-4189/© 2026 JSAA. All Rights Reserved.

Journal Homepage

<https://pub.scientificirg.com/index.php/JSAA>



Automating COVID-19 Classification in Chest CT Scans Using Advanced CNN Architectures

Muhammad GamalEldin^{a1}, Hala Abdel Galil^b, Hatem M. Noaman^a, Hamdi A. Mahmoud^a

^a Faculty of Computers and Artificial Intelligence, Beni-Suef University, Beni-Suef City, 62511, Egypt. Emails: mohamed.gamal@fcis.bsu.edu.eg , hnoaman@fcis.bsu.edu.eg , Dr_hamdimahmoud@yahoo.com

^b Faculty of Computers and Artificial Intelligence, Helwan University, Helwan City, 11731, Egypt. Email: Hala.nagy@fei.helwan.edu.eg

ABSTRACT

This paper proposes an efficient and fully automated method for classifying COVID-19 using CT scan images of a patient's chest. The study utilizes the publicly available SARS-CoV-2 CT scan dataset, which contains 1252 CT scans positive for SARS-CoV-2 (COVID-19) infection, 1230 CT scans from SARS-CoV-2-negative patients, and a total of 2482 cross-sectional scans. This research explores various topologies designed to enhance the classification accuracy of convolutional neural networks, particularly when dealing with images containing small objects of interest. DenseNet169 is particularly effective in handling small-sized infection patterns commonly observed in COVID-19 cases, as it allows the model to analyze images at varying resolutions effectively without compromising small-object data integrity. Several approaches were evaluated, including VGG19, Xception, ResNet101, DenseNet169, and two custom models: a "custom vanilla" model based on the vanilla architecture and a "custom inception" model based on the inception architecture. Among these, DenseNet169 achieved the highest performance, attaining an impressive accuracy rate of 99.731%.

PAPER INFORMATION

HISTORY

Received: 2 January 2026

Revised: 17 March 2026

Accepted: 19 April 2026

Online: 24 April 2026

MSC:

68T07; 68R10; 94A60;
68M15

KEYWORDS

**Convolutional Networks;
COVID-19;
CT scan of the lungs;
DenseNet169;
SARS-CoV.**

¹Corresponding author: Faculty of Computers and Artificial Intelligence, Beni-Suef University, Beni-Suef City, 62511, Egypt . Email: mohamed.gamal@fcis.bsu.edu.eg

1. INTRODUCTION

Since December 2019, a previously unknown coronavirus, referred to as the novel coronavirus (2019-nCoV or COVID-19), has been discovered in Wuhan, China. Subsequently, COVID-19 rapidly spread across China and worldwide, causing symptoms such as fever, respiratory distress, coughing, and invasive lesions in both lungs of affected individuals [1]. This pivotal moment marked the beginning of a global effort to understand, combat, and manage the unprecedented challenges posed by the COVID-19 pandemic. Coronaviruses are a large family of viruses capable of causing illnesses in both animals and humans. In humans, several coronaviruses are known to cause

respiratory infections, ranging from mild conditions similar to the common cold to more severe and potentially fatal diseases, such as Middle East Respiratory Syndrome (MERS) and Severe Acute Respiratory Syndrome (SARS). The most recently discovered coronavirus causes the disease known as COVID-19. This novel virus has introduced unique challenges to global health, requiring coordinated efforts to understand and mitigate its spread. Prior to the outbreak in Wuhan, China, in December 2019, both this virus and the associated disease were entirely unknown. Since its emergence, COVID-19 has rapidly evolved into a global pandemic, affecting numerous countries worldwide [2]. On January 30, 2020, the World Health Organization (WHO) declared a global health emergency [3]. Typical symptoms of COVID-19 include fever, cough, and difficulty breathing [5, 9]. Although most cases result in mild symptoms, some progress to viral pneumonia. As of August 7, 2020, more than 19 million confirmed cases had been reported worldwide, spanning nearly every region, with 717,687 documented deaths [4]. After an extended period of quarantine, several nations are taking the initial steps toward DE confinement strategies [6, 7]. However, the death toll from COVID-19 continues to rise, particularly in the United States, the United Kingdom, and Brazil [4]. In response to this ongoing crisis, innovative technologies and strategies have emerged to strengthen healthcare systems during the pandemic [8]. Radiologists have played a key role in supporting the use of CT scans and X-rays for detecting COVID-19, helping to develop methods that incorporate these imaging tools into the diagnostic process. This approach emphasizes the importance of medical imaging in assessing and managing COVID-19 cases. Most patients with symptoms of COVID-19 undergo X-rays and CT scans of their lungs after at least four days, which reveal signs of infection and confirm the presence of the virus in their bodies [10]. Between January 6 and February 6, 2020, a total of 1,014 patients underwent chest CT scans and RT-PCR testing. Using RT-PCR as the reference standard, a comparative analysis indicated that chest CT may serve as a valuable tool for detecting COVID-19 in endemic areas [10]. While medical imaging is not recommended as a definitive diagnostic method, it can support early COVID-19 detection due to the limitations of other diagnostic approaches [11]. Furthermore, the shortage of diagnostic kits in many heavily affected areas worldwide has prompted researchers to develop new and simpler methods for diagnosing the disease. These efforts aim to address the urgent need for more accessible and rapid testing solutions, particularly in resource-limited settings where the demand for testing remains high. Innovations in diagnostic approaches continue to play a crucial role in the ongoing fight against the COVID-19 pandemic. CT scanning has emerged as a pivotal tool in the clinical diagnosis of COVID-19 patients [2]. Due to the availability of medical imaging devices in most treatment centers, researchers analyze CT scans and X-rays to detect COVID-19. In many patients with COVID-19, infections are observed in the lungs, which can aid in diagnosing the disease. Analysis of CT scans in COVID-19 patients revealed pneumonia caused by the novel coronavirus [1]. In studies referenced as [10] and [12], it was observed that CT scans of some patients with early-onset COVID-19 symptoms revealed additional coronavirus infections. Their RT-PCR test results were negative at the time, but after both tests were repeated a few days later, RT-PCR confirmed the CT scan's diagnostic findings. This highlights the potential utility of medical imaging, particularly CT scans, as a primary diagnostic tool for COVID-19 in the early stages of the illness. It can assist in isolating and managing suspected cases promptly, thereby reducing the risk of viral transmission. However, it is important to note that medical imaging alone is not recommended for a definitive diagnosis, and confirmation through other means is typically necessary for conclusive identification of COVID-19.

2. RELATED WORK

Recently, several machine learning and deep learning techniques have been applied to classify COVID-19 using CT scan images. For instance, Li et al. [27] developed a deep learning model named COVNet to extract visual features from chest CT scans for detecting COVID-19. These visual features were utilized to differentiate between community-acquired pneumonia and other non-pneumonia lung diseases. However, COVNet could not categorize the severity of the disease. Horry et al. [28] proposed a COVID-19 detection method based on transfer learning and multimodal image data. Unfortunately, the performance of the resulting classification model was poor. Wang et al. [29] introduced a 3D deep convolutional neural network called DecoVNet to detect COVID-19 from CT volumes, achieving an accuracy of 90.1%. However, the dataset used was small, comprising only 630 images: 499 CT volumes for training and 131 for testing, which resulted in an unbalanced dataset. Han et al. [30] proposed an attention-based

deep 3D multi-instance learning (AD3D-MIL) model that achieved an accuracy of 97.9% using 460 chest CT examples. Nevertheless, the dataset size was insufficient for training deep learning techniques effectively. Similarly, Ouyang et al. [31] introduced a novel online attention module integrated with a 3D convolutional neural network (CNN) to focus on infection regions in the lungs for diagnostic decisions. This model achieved an accuracy of 87.5% using 2796 chest CT examples. Pathak et al. [32] proposed a deep bidirectional long-term memory network combined with a density mixture network model (DBM). To optimize the DBM model's hyperparameters, they employed the Memetic Adaptive Differential Evolution (MADE) algorithm. Using 1790 Chest CT examples, their model achieved an accuracy of 98.37%. Yu-Dong et al. [33] developed a deep convolutional neural network (DCNN) model, which achieved an accuracy of $93.64 \pm 1.42\%$ using 640 chest CT examples. However, the dataset was small. Soares [13] presented a multiclass CT scan dataset for identifying SARS-CoV-2, the virus responsible for COVID-19. The dataset contained 4173 CT scans from 210 patients, including 2168 scans from 80 patients confirmed to be SARS-CoV-2-positive through RT-PCR testing. A smaller version of this dataset, consisting of 2482 CT scans, was also used. Using the xDNN model, an accuracy of 97.31% was achieved. Owida et al. [35] proposed a hybrid approach for classifying chest X-ray images by extracting features using both wavelet transforms and Mel Frequency Cepstral Coefficients (MFCCs), followed by classification using a Support Vector Machine (SVM) model. Their method demonstrated promising performance, achieving an overall accuracy of 94.13% in distinguishing between normal and pathological chest X-rays. **Table 1.** provides an overview of the methods and quantitative results for COVID-19 classification.

Table 1. Overview of methods and quantitative results toward COVID-19 classification

| Author | Data Set | No. of Images | Method | Quantitative results indicators | Date of publication |
|---------------|------------------------------|---------------|---|---------------------------------|---------------------|
| Lin Li [27] | Internal | 4352 | 3D CNN | AUC= 95%; | 19 Mar 2020 |
| J. HORRY [28] | COVID-CT Dataset | 746 | VGG19 | Acc = 84% | 14 August 2020 |
| Wang [29] | Internal | 630 | 3D CNN | Acc = 90.1% ; | 8 AUGUST 2020 |
| Han [30] | Internal | 460 | Attention mechanism + 3D multiple instance learning | Acc =97.9%; AUC=99.0% | 8 AUGUST 2020 |
| Ouyang [31] | Internal | 2796 | Attention mechanism + 3D CNN | Acc = 87.5%; AUC= 94.4%; | 8 AUGUST 2020 |
| Pathak [32] | Chest CT images | 1790 | DBM | Acc = 98.37%; AUC= 98.32% | 20 July 2020 |
| Yu-Dong[33] | Internal | 640 | DCNN | Acc = $93.64 \pm 1.42\%$ | 3 November 2020 |
| A. Waheed[34] | COVID-19 chest X-ray dataset | 932 | VGG16 + ACGAN | Acc = 95% | 8 Mar 2021 |
| Soares [13] | SARS-CoV-2 CT scan dataset | 4173 | xDNN | Acc = 97.31% | 27 June 2023 |

Internal: nonpublic dataset

These studies vary in their use of datasets, evaluation metrics, and implementation techniques, which may result in different levels of accuracy and reliability. Unlike many existing studies, this paper provides a comprehensive comparison of six well-known convolutional neural network (CNN) architectures using the same publicly available

CT scan dataset. While prior works often focus on a single model or a custom architecture, our study offers a fair benchmarking environment across multiple pre-trained models, including DenseNet169, which demonstrated superior performance. Additionally, we propose a custom lightweight CNN architecture that balances accuracy and computational efficiency. Our work also provides deeper training analysis through learning curves and performance metrics such as precision, sensitivity, and specificity, which are often overlooked in similar studies. These aspects highlight the novelty and practical relevance of our contribution in the context of COVID-19 CT image classification.

3. MATERIALS AND METHODS

3.1. SARS-COV-2 CT-Scan Dataset

The SARS-CoV-2 CT scan dataset, publicly released by Soares et al. [13], contains 2482 CT images collected from real patients in hospitals across São Paulo, Brazil. The dataset includes 1252 images from COVID-19-positive patients and 1230 from negative cases. The data were preprocessed by resizing to a standard dimension, normalizing pixel values, and applying data augmentation techniques such as horizontal/vertical flipping to improve generalization. The dataset was split into 70% training (1737 images), 15% validation, and 15% testing subsets. Figure 1 provides visual examples of positive and negative samples.

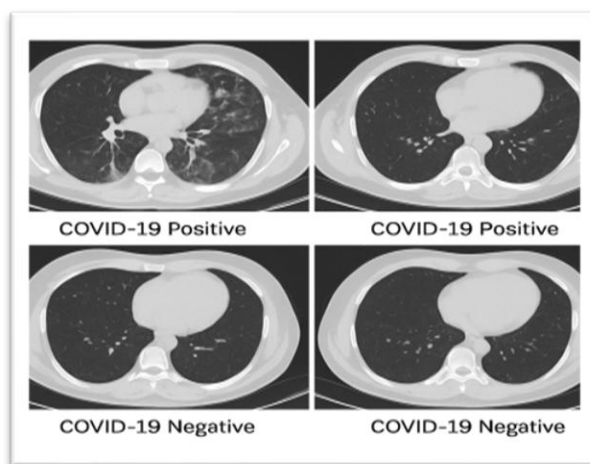


Figure 1. Samples of Infected and non-infected Images from the Data set

3.2. Enhanced deep convolutional neural network for classification

Computer vision systems can analyze medical images such as CT scans, X-rays, MRIs, mammograms, etc., with greater accuracy and speed [15]. Because a computer vision system can analyze medical images much faster, it can significantly reduce the workload of radiologists by allowing them to treat more patients. This can also reduce burnout rates for radiologists, which have been rising amidst the industry challenges. This can also be helpful in remote areas where the supply of radiologists is limited; computer vision systems can assist existing radiologists in managing more patients [15]. Implementing computer vision methods on deep neural networks, especially using the convolution layers, has resulted in extremely accurate performance. This paper proposes convolution networks to classify the SARS-CoV-2 CT-Scan Dataset into normal or COVID-19. We trained, evaluated, and compared six different deep convolutional networks: ResNet101 [16], DenseNet169[17], Xception [18], VGG19[19], and two custom models (CNN based on vanilla, CNN based on inception) as shown in **Figure 2**.

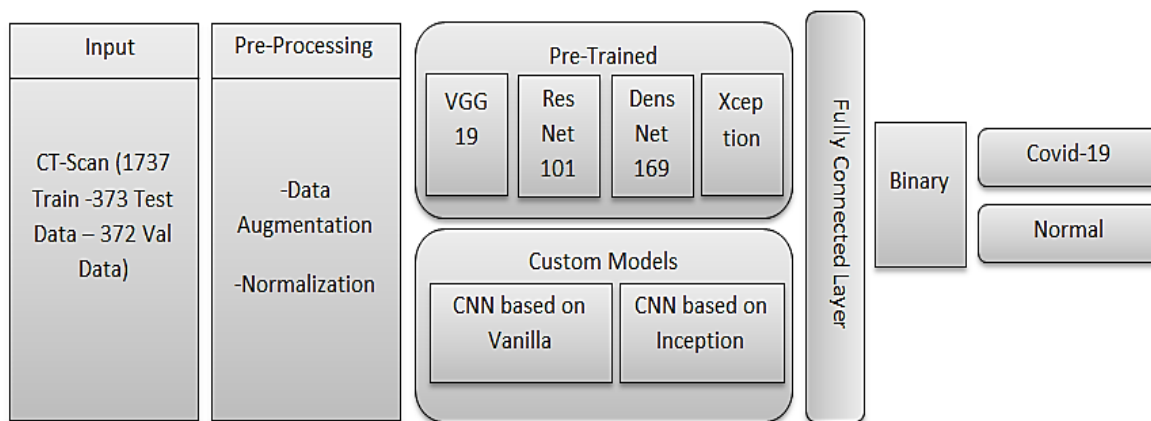


Figure 2. Illustration of the pipeline of the proposed methods

Convolutional neural network (CNN), a class of artificial neural networks that has become dominant in various computer vision tasks, is attracting interest across a variety of domains, including radiology. CNN is designed to automatically and adaptively learn spatial hierarchies of features through backpropagation by using multiple building blocks, such as convolution layers, pooling layers, and fully connected layers [14].

For conventional deep learning networks, they usually have conv-layers then fully connected (FC) layers for classification task like AlexNet, ZFNet and VGGNet, without any skip / shortcut connection. We call them plain networks. When the plain network is deeper (i.e. layers are increased), the problem of vanishing/exploding gradients occurs [20].

VGG-19 is a convolutional neural network (CNN) architecture that was proposed by the Visual Geometry Group (VGG) at the University of Oxford. It is a deeper version of the VGG network, specifically consisting of 19 layers. The VGG-19 architecture is known for its simplicity and uniformity, with convolutional layers of a small filter size (3x3) and max-pooling layers (2x2) applied throughout the network.

VGG-19 consists of a series of convolutional blocks. Each block consists of two or more convolutional layers followed by a max pooling layer. The convolutional layers have a filter size of 3x3 and a stride of 1, and they apply padding to maintain the spatial dimensions. The max pooling layers have a pooling size of 2x2 and a stride of 2, which reduces the spatial dimensions by half. Block 1 has 2 convolutional layers with 64 filters and block 2 has 2 convolutional layers with 128 filters and block 3 has 4 convolutional layers with 256 filters and block 4 has 4 convolutional layers with 512 filters and block 5 has 4 convolutional layers with 512 filters and Fully Connected Layers: After the convolutional blocks, VGG-19 has three fully connected layers. Each fully connected layer consists of 4096 neurons as shown in **Figure 3**.

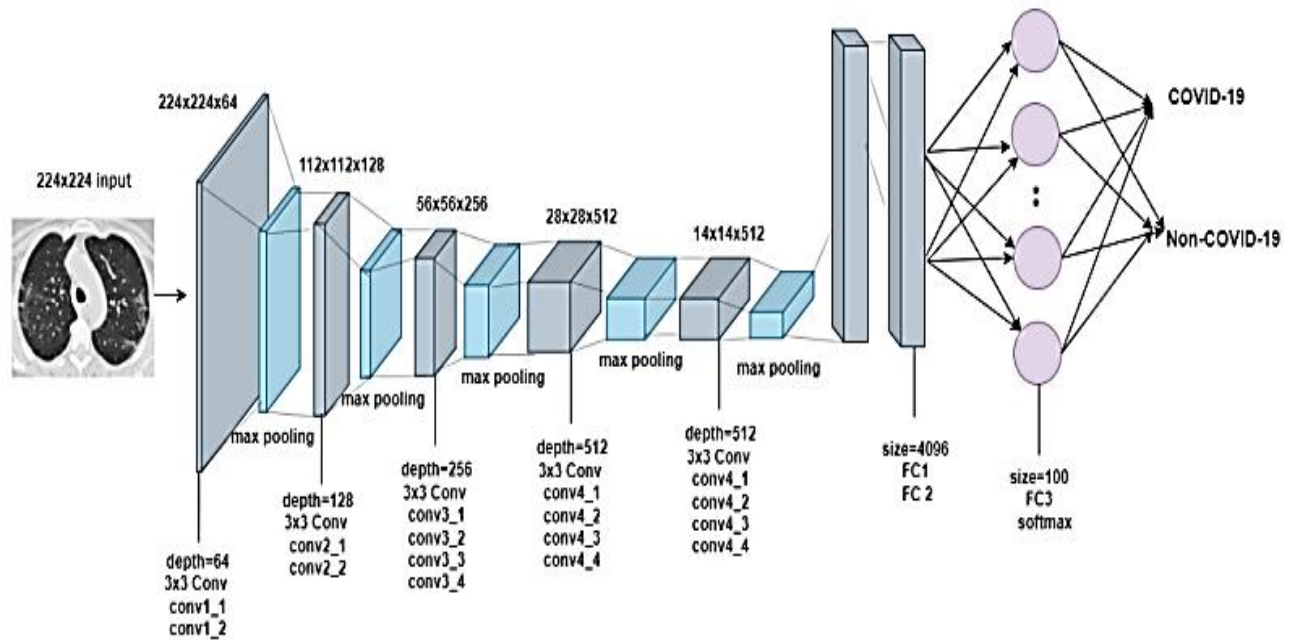


Figure 3. Proposed VGG19 COVID-19 classification architecture

ResNet can have a very deep network of up to 152 layers by learning the residual representation functions instead of learning the signal representation directly [20].

ResNet introduces a skip connection (or shortcut connection) to fit the input from the previous layer to the next layer without any modification of the input. Skip connection enables having a deeper network, and finally, ResNet becomes the Winner of ILSVRC 2015 in image classification, detection, and localization, as well as the winner of MS COCO 2015 detection and segmentation [20].

One of the problems ResNets solves is the famous vanishing gradient. This is because when the network is too deep, the gradients from where the loss function is calculated easily shrink to zero after several applications of the chain rule. This results in the weights never updating their values and therefore, no learning is being performed. With ResNets, the gradients can flow directly through the skip connections backwards from later layers to initial filters [21].

ResNet-101 is a convolutional neural network that is 101 layers deep. You can load a pretrained version of the network trained on more than a million images from the ImageNet [24] database. The ResNet101 model is a deep residual network that allows for better performance by utilizing skip connections to mitigate the vanishing gradient problem. **Figure 4** illustrates the architecture of ResNet101 used in this work.

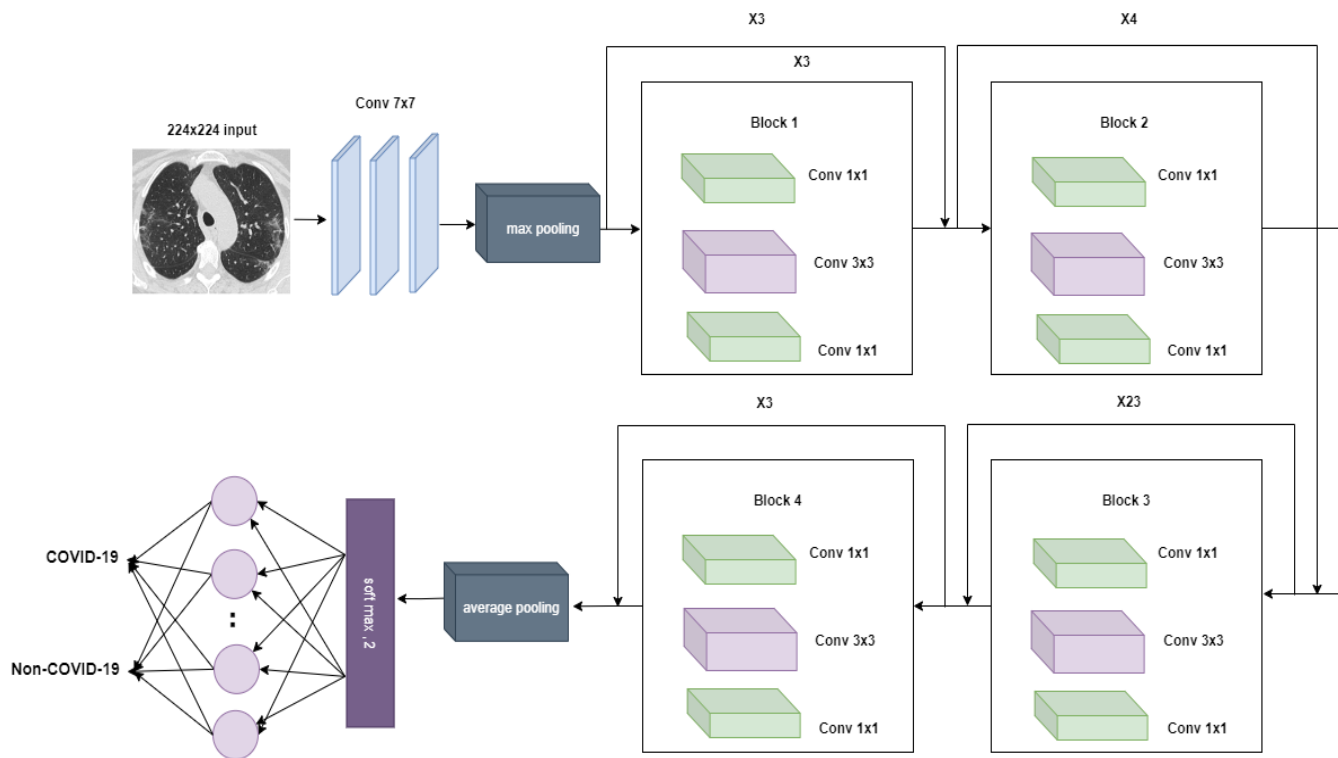


Figure 4. ResNet101 architecture

DenseNet is one of the new discoveries in neural networks for visual object recognition. DenseNet is quite similar to ResNet with some fundamental differences. ResNet uses an additive method (+) that merges the previous layer (identity) with the future layer, whereas DenseNet concatenates (.) the output of the previous layer with the future layer [22].

DenseNet was developed specifically to improve the declined accuracy caused by the vanishing gradient in high-level neural networks. In simpler terms, due to the longer path between the input layer and the output layer, the information vanishes before reaching its destination [22].

DenseNets have several compelling advantages: they alleviate the vanishing-gradient problem, strengthen feature propagation, encourage feature reuse, and substantially reduce the number of parameters [17].

The DenseNet -169 model is one of the DenseNet group of models designed to perform image classification as shown in **Figure 5**. The main difference with the densenet-121 model is the size and accuracy of the model [23]

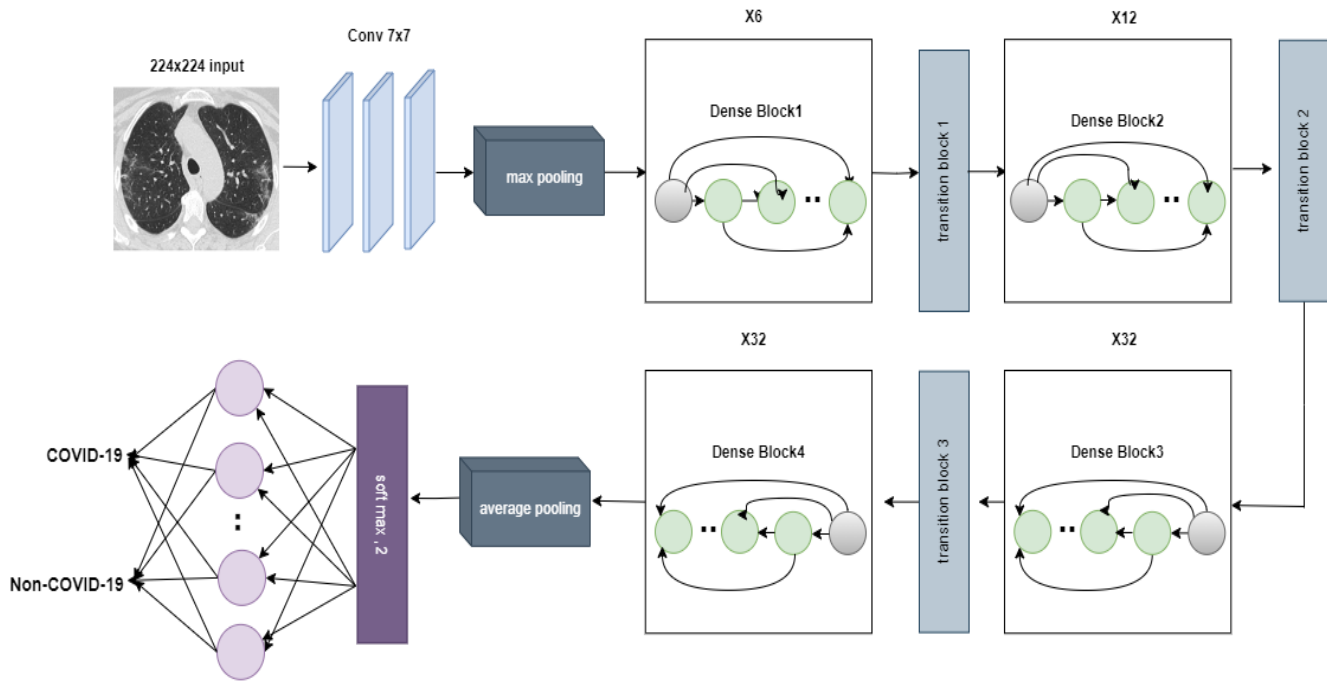


Figure 5. DesNet169 architecture

Xception introduced new inception modules constructed of depth-wise, separable convolution layers (depth-wise convolutional layers followed by a point-wise convolution layer). Xception achieved one of the best results on the ImageNet dataset.

The proposed model, based on vanilla architecture, consists of a convolution layer, maximum pooling, batch normalization, and a classification layer. The network architecture consists of three 3x3 convolution layers with 16,32, and 64 units, respectively, and three maximum pooling layers of 2x2 sizes. There are also three batch normalization layers, as shown in Figure 6. Proposed model structure parameters are shown in Table 2.

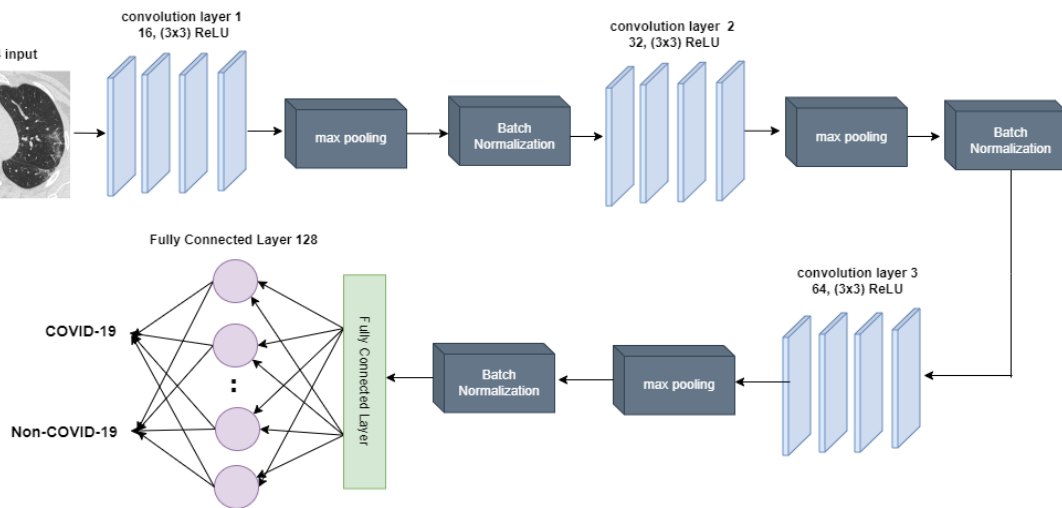


Figure 6. CNN based on Vanilla.

Table 2. Proposed Model Parameters.

| Layer (type) | Output Shape | Parameter |
|---------------------------------|--------------|-----------|
| | Conv2D | 22x22x16 |
| MaxPooling2D | 11x11x16 | 0 |
| BatchNormalization | 11x11x16 | 64 |
| Conv2D | 109x109x32 | 4640 |
| MaxPooling2D | 54x54x32 | 0 |
| BatchNormalization | 54x54x32 | 128 |
| Conv2D | 52x52x64 | 18496 |
| MaxPooling2D | 52x52x64 | 0 |
| BatchNormalization | 52x52x64 | 256 |
| Flatten | 173056 | 0 |
| Dense | 128 | 22151296 |
| Dense | 2 | 258 |
| Total Parameters: 22,175,586 | | |
| Trainable Parameters:22,175,362 | | |
| Non-Trainable Parameters: 224 | | |

For the proposed model based on the Inception architecture, five layers are applied as shown in **Figure 7**.

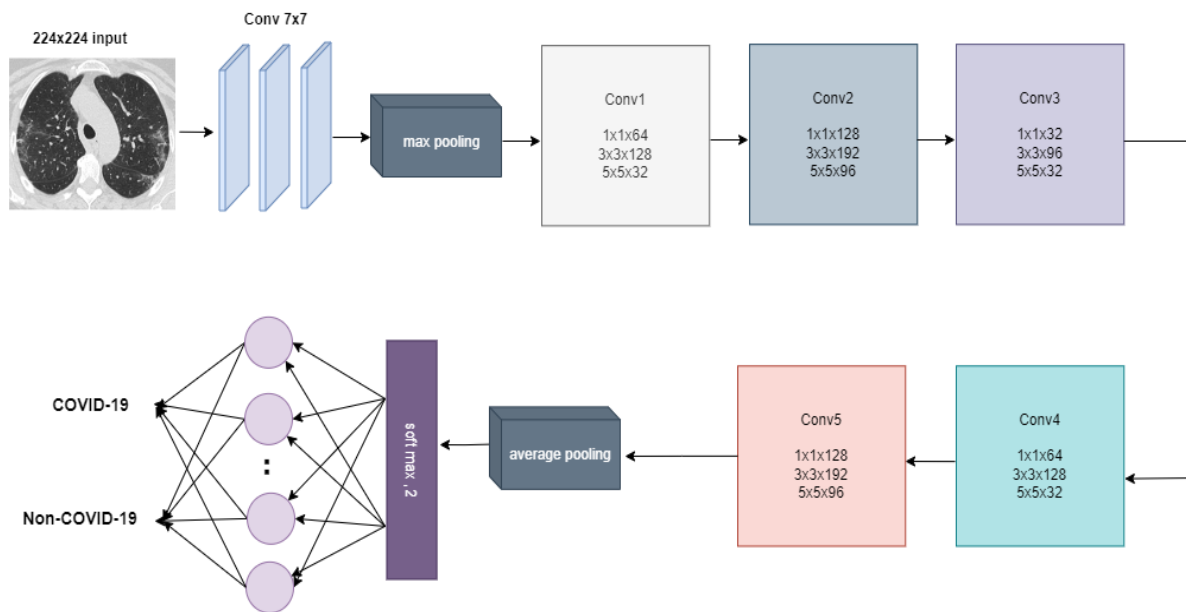


Figure 7. CNN based on Inception.

3.3. Training Phase

We separated the dataset into training, validation, and testing data. The training data has 70% of the total data set, about 1737 images, while the validation and testing data have 30% data set.

We trained our dataset on VGG19, ResNet101, DensNet169, Xception, and our model. For training the networks, we used transfer learning from the ImageNet [24] pre-trained weights to make the networks' convergence faster. We chose the Adamax optimizer and the Categorical Cross-entropy loss function. We also used data augmentation methods to make learning more efficient and stop the network from overfitting. Our training parameters are listed in Table 3.

Table 3. Training Parameters

| Training parameters | Models | | | | |
|------------------------------|--------------------------|--------------------------|--------------------------|--------------------------|----------------------------|
| | VGG19 | ResNet101 | Xception | DensNet169 | Custom model-based vanilla |
| Learning Rate | 0.001 | 0.001 | 0.001 | 0.001 | 0.001 |
| Batch size | 14 | 16 | 14 | 16 | 16 |
| Optimizer | Adamax | Adamax | Adamax | Adamax | Adam |
| Loss function | categorical_crossentropy | categorical_crossentropy | categorical_crossentropy | categorical_crossentropy | binary_crossentropy |
| Epochs | 55 | 23 | 10 | 18 | 42 |
| Horizontal/vertical flipping | yes | yes | yes | yes | yes |

4. EXPERIMENTAL RESULTS

This section reports the Image classification results of the trained networks on the test set images. We used the Keras library [25] on the Tensorflow backend [26] for developing and running the deep networks.

4.1. Image Classification Results

We trained each network on the training set with the explained parameters in Section 2.3. We also used the accuracy metric while training for monitoring the network validation result after each epoch to find the training network's best converged version.

We evaluated the trained networks using four different metrics for each of the classes and the overall accuracy for all the classes as follows:

$$\text{Accuracy (for each class)} = \frac{TP+TN}{TP+FP+TN+FN} \quad (1)$$

$$\text{Specificity} = \frac{TN}{TN+FP} \quad (2)$$

$$\text{Sensitivity} = \frac{TP}{TP+FN} \quad (3)$$

$$\text{Precision} = \frac{TP}{TP+FP} \quad (4)$$

In these equations, for each class, TP (True Positive) is the number of correctly classified images, FP (False Positive) is the number of the wrong classified images, FN (False Negative) is the number of images that have been detected as a wrong class, and TN (True Negative) is the number of images that do not belong to another class and have not been classified as that class.

In this study, DenseNet169 achieved an accuracy of 99.731%, Resnet101 achieved an accuracy of 98.79, VGG19 achieved an accuracy of 94.77, Xception achieved an accuracy of 99.59 %, Custom model based on vanilla achieved an accuracy of 95.97 %, and Custom model on inception achieved an accuracy of 95.71%.

After training the DenseNet169 model, it gave high results in the training and validation phases. Specifically, the accuracy in the train phase was 100%, while in the validation phase, it was 99.731%. The loss was 0.0 and 0.01588 in the training and the validation.

The accuracy and loss plots of all six models are shown in **Figures 8–11**.

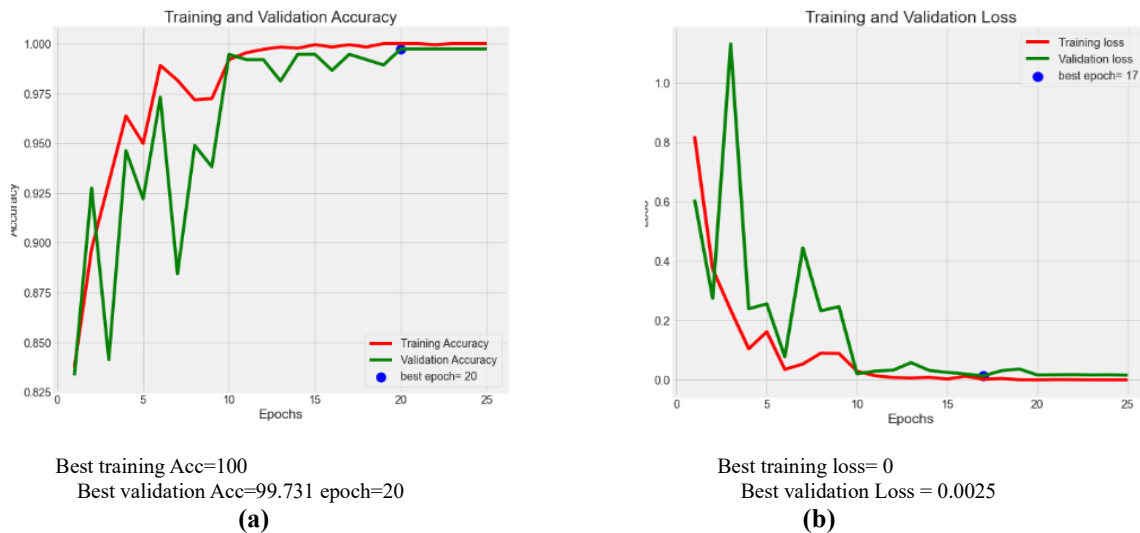
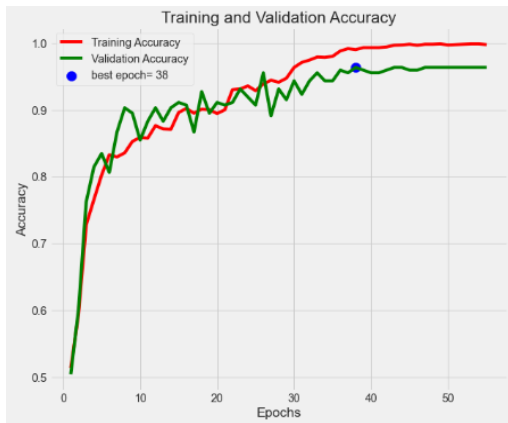


Figure.8. (a) Accuracy and (b) loss plots throughout the training process of the Dense169 model



Best training Acc=99.04
Best validation Acc=96.371 epoch=38

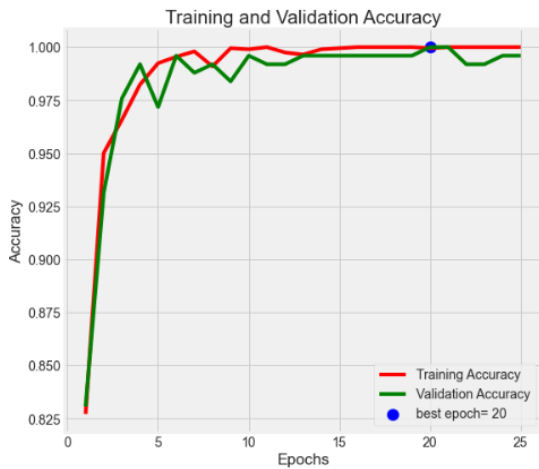
(a)



Best training Loss = 0.033
Best validation Loss = 0.19392 epoch=38

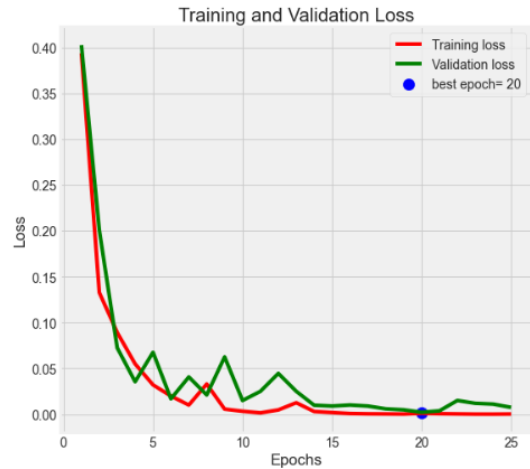
(b)

Figure.9. (a) Accuracy and (b) loss plots throughout the training process of the VGG19 model.



Best training Acc=.9959
Best validation Acc=100 epoch=20

(a)



Best training Loss= 0.001
Best validation Loss = 0.00212

(b)

Figure.10. (a) Accuracy and (b) loss plots throughout the training process of the Xception model

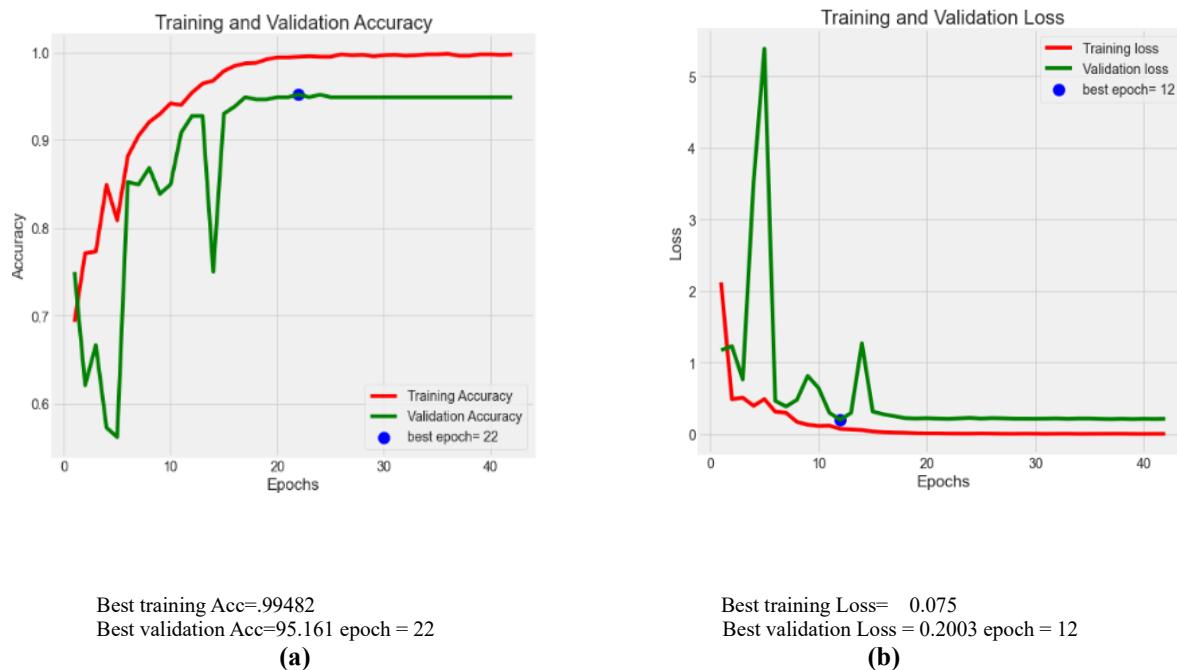


Figure.11. (a) Accuracy and (b) loss plots throughout the training process of the Custom model

5. DISCUSSION

The Proposed model evaluation results are shown in **Table 4**. The results show that DensNet169 achieved 99.731% overall accuracy for the COVID-19 class. VGG19 evaluation results show 94.77% overall accuracy. ResNet101 evaluation results show 98.79% overall accuracy. Xception evaluation results show 99.59% overall accuracy. Custom model based on vanilla evaluation results show 95.97% overall accuracy. Custom model based on inception evaluation results show 95.71% overall accuracy. Our investigations indicate that DensNet169 detects infection points very carefully, but normal models like VGG19 and ResNet169 determine any similar points as infections and mistakenly identify more normal images as COVID.

Table 4. Evaluation Results for Each Network

| Network | Evaluation Results | | | | | | |
|-------------------------------|-----------------------------|---------------------------|--------------------------|----------------------|------------------------------|-----------------------|--------|
| | Correctly classified images | Wrongly classified images | COVID correct classified | COVID not classified | Normal, correctly classified | Normal not classified | Acc |
| VGG19 | 236 | 13 | 120 | 6 | 116 | 7 | 94.77% |
| ResNet101 | 246 | 3 | 124 | 2 | 122 | 1 | 98.79% |
| Xception | 248 | 1 | 126 | 0 | 122 | 1 | 99.59% |
| DensNet169 | 370 | 1 | 187 | 1 | 182 | 0 | 99.73% |
| Custom model based on vanilla | 358 | 15 | 177 | 11 | 181 | 4 | 95.97% |
| Custom model on inception | 373 | 16 | 183 | 5 | 174 | 11 | 95.71% |

Table 4 provides a breakdown of classification performance for each tested model. ‘Correct classified images’ and ‘Wrong classified images’ represent the total predictions. ‘COVID correctly classified’ indicates how many infected cases were correctly detected, while ‘COVID not classified’ indicates missed COVID-positive cases. Similarly, ‘Normal correctly classified’ and ‘Normal not classified’ reflect performance on healthy cases. The accuracy column summarizes overall classification accuracy.

6. CONCLUSION

In this paper, a COVID-19 disease classification model is proposed to classify the infected patients from chest CT images. Initially, the chest CT dataset of COVID-19-infected patients is decomposed into training, validation, and testing groups. The training dataset is utilized for building the COVID-19 disease classification model. The proposed MODEL-based CNN and competitive classification models are applied to the training data. Finally, the comparisons are drawn between VGG19, ResNet101, Xception, DensNet169, a custom model based on vanilla, and a custom model on inception. DensNet169 obtained the best result, 99.731% overall accuracy. Based on the results obtained, it can be understood that the proposed methods can improve COVID-19 classification and run fast enough for implementation in medical centers. Unlike many previous works, our study evaluates multiple CNN architectures under consistent conditions, uses a well-curated dataset, and introduces a customized lightweight CNN. The use of DenseNet169 in particular demonstrated superior accuracy while maintaining computational efficiency.

ACKNOWLEDGMENT

We would like to express our heartfelt gratitude to our colleagues and mentors for their invaluable guidance and constructive feedback throughout this research. We also extend our thanks to the institutions and organizations that provided the necessary resources and support to make this study possible. Special appreciation goes to the healthcare professionals and data providers who made the datasets accessible for academic research, enabling the advancement of COVID-19 detection techniques.

REFERENCES

- [1] F. Song et al., "Emerging 2019 novel coronavirus (2019-nCoV) pneumonia," *Radiology*, vol. 295, no. 1, pp. 210–217, 2020.
- [2] World Health Organization, "Coronavirus disease (COVID-19)," [Online]. Available: <https://www.who.int/westernpacific/health-topics/detail/coronavirus>. [Accessed: Mar. 20, 2023].
- [3] K. G. Andersen et al., "The proximal origin of SARS-CoV-2," *Nat. Med.*, vol. 26, no. 4, pp. 450–452, 2020.
- [4] E. Dong, H. Du, and L. Gardner, "An interactive web-based dashboard to track COVID-19 in real time," *Lancet Infect. Dis.*, 2020.
- [5] W. J. Guan et al., "Clinical characteristics of coronavirus disease 2019 in China," *N. Engl. J. Med.*, vol. 382, no. 18, pp. 1708–1720, 2020.
- [6] M. Salathé et al., "COVID-19 epidemic in Switzerland: On the importance of testing, contact tracing and isolation," *Swiss Med. Wkly*, vol. 150, 2020.
- [7] S. Cousins, "New Zealand eliminates COVID-19," *Lancet*, vol. 395, no. 10235, p. 1474, 2020.
- [8] Z. Hu et al., "Artificial intelligence forecasting of COVID-19 in China," *arXiv:2002.07112*, 2020.
- [9] Z. Xu et al., "Pathological findings of COVID-19 associated with acute respiratory distress syndrome," *Lancet Respir. Med.*, vol. 8, no. 4, pp. 420–422, 2020.
- [10] T. Ai et al., "Correlation of chest CT and RT-PCR testing for COVID-19 in China: A report of 1014 cases," *Radiology*, vol. 296, no. 2, pp. E32–E40, 2020.
- [11] American College of Radiology, "ACR recommendations for the use of chest radiography and CT for suspected COVID-19 infection," [Online]. Available: <https://www.acr.org>. [Accessed: Mar. 20, 2023].
- [12] X. Xie et al., "Chest CT for typical coronavirus disease 2019 pneumonia: Relationship to negative RT-PCR testing," *Radiology*, vol. 296, no. 2, pp. E41–E45, 2020.
- [13] E. Soares et al., "A large multiclass dataset of CT scans for COVID-19 identification," *Evolving Systems*, pp. 1–6, 2023.

- [14] R. Yamashita et al., "Convolutional neural networks: An overview and application in radiology," *Insights Imaging*, vol. 9, pp. 611–629, 2018.
- [15] AIMultiple, "Computer vision in radiology in 2023: Benefits & challenges," [Online]. Available: <https://research.aimultiple.com/computer-vision-radiology/>. [Accessed: May 20, 2023].
- [16] K. He et al., "Identity mappings in deep residual networks," in *Proc. ECCV*, 2016, pp. 630–645.
- [17] G. Huang et al., "Densely connected convolutional networks," in *Proc. CVPR*, 2017, pp. 4700–4708.
- [18] F. Chollet, "Xception: Deep learning with depthwise separable convolutions," in *Proc. CVPR*, 2017, pp. 1251–1258.
- [19] K. Simonyan and A. Zisserman, "Very deep convolutional networks for large-scale image recognition," *arXiv:1409.1556*, 2014.
- [20] Towards Data Science, "Review: ResNet — Winner of ILSVRC 2015," [Online]. Available: <https://towardsdatascience.com>. [Accessed: Aug. 1, 2023].
- [21] Towards Data Science, "Understanding and visualizing ResNets," [Online]. Available: <https://towardsdatascience.com>. [Accessed: Aug. 1, 2023].
- [22] Pluralsight, "Introduction to DenseNet with TensorFlow," [Online]. Available: <https://www.pluralsight.com>. [Accessed: Aug. 1, 2023].
- [23] OpenVINO, "DenseNet-169 model," [Online]. Available: <https://docs.openvino.ai>. [Accessed: Aug. 1, 2023].
- [24] J. Deng et al., "ImageNet: A large-scale hierarchical image database," in *Proc. CVPR*, 2009, pp. 248–255.
- [25] F. Chollet, "Keras," 2015.
- [26] M. Abadi et al., "TensorFlow: Large-scale machine learning on heterogeneous distributed systems," *arXiv:1603.04467*, 2016.
- [27] L. Li et al., "Artificial intelligence distinguishes COVID-19 from community-acquired pneumonia on chest CT," *Radiology*, 2020.
- [28] M. J. Horry et al., "COVID-19 detection through transfer learning using multimodal imaging data," *IEEE Access*, vol. 8, pp. 149808–149824, 2020.
- [29] X. Wang et al., "A weakly-supervised framework for COVID-19 classification and lesion localization from chest CT," *IEEE Trans. Med. Imaging*, vol. 39, no. 8, pp. 2615–2625, 2020.
- [30] Z. Han et al., "Accurate screening of COVID-19 using attention-based deep 3D multiple instance learning," *IEEE Trans. Med. Imaging*, vol. 39, no. 8, pp. 2584–2594, 2020.
- [31] X. Ouyang et al., "Dual-sampling attention network for diagnosis of COVID-19," *IEEE Trans. Med. Imaging*, vol. 39, no. 8, pp. 2595–2605, 2020.
- [32] Y. Pathak et al., "Deep bidirectional classification model for COVID-19 patients," *IEEE/ACM Trans. Comput. Biol. Bioinform.*, vol. 18, no. 4, pp. 1234–1241, 2020.
- [33] Y. D. Zhang et al., "A five-layer deep CNN with stochastic pooling for COVID-19 diagnosis," *Mach. Vis. Appl.*, vol. 32, pp. 1–13, 2021.
- [34] A. Waheed et al., "CovidGAN: Data augmentation using auxiliary classifier GAN for improved COVID-19 detection," *IEEE Access*, vol. 8, pp. 91916–91923, 2020.
- [35] H. A. Owida et al., "Classification of chest X-ray images using wavelet and MFCC features," *Eng. Technol. Appl. Sci. Res.*, vol. 11, no. 4, pp. 7296–7301, 2021.